

Application of the Monte Carlo Shell Model to *Ab Initio* No-Core Calculations

T. Abe^a, P. Maris^b, T. Otsuka^{a,c,d}, N. Shimizu^c, Y. Utsuno^e
and J. P. Vary^b

^a*Department of Physics, the University of Tokyo, Hongo, Tokyo 113-0033, Japan*

^b*Department of Physics and Astronomy, Iowa State University, Ames, Iowa 50011, USA*

^c*Center for Nuclear Study, the University of Tokyo, Hongo, Tokyo 113-0033, Japan*

^d*National Superconducting Cyclotron Laboratory, Michigan State University, East Lansing, Michigan 48824, USA*

^e*Advanced Science Research Center, Japan Atomic Energy Agency, Tokai, Ibaraki 319-1195, Japan*

Abstract

We report recent developments of the Monte Carlo Shell Model (MCSM) and its application to the no-core calculations. It is shown that recent developments enable us to apply the MCSM to the shell-model calculations without a core. Benchmarks between the MCSM and Full-Configuration Interaction (FCI) methods demonstrate consistent results with each other within estimated uncertainties. No-Core Full Configuration (NCFC) results are also presented as full *ab initio* solutions extrapolated to the infinite basis limit.

Keywords: *Shell model; Monte Carlo shell model; ab initio approaches*

1 Introduction

One of the major challenges in nuclear physics is to understand nuclear structure and reactions from *ab initio* calculations. Such calculations have recently become feasible for nuclear many-body systems beyond $A = 4$ due to the rapid evolution of computational technologies. Together with the Green's Function Monte Carlo [1] and Coupled Cluster theory [2], the No-Core Shell Model (NCSM) is one of the relevant *ab initio* methods and has been emerging for about a decade. It is now available for the study of nuclear structure and reactions in the p -shell nuclei [3].

As the NCSM treats all the nucleons democratically, computational demands for the calculations explode exponentially as the number of nucleons increases. Current computational resources limit the direct diagonalization of the Hamiltonian matrix using the Lanczos algorithm to basis spaces with a dimension of around 10^{10} . In order to access heavier nuclei beyond the p -shell region with larger basis dimensions, many efforts have been devoted to the NCSM calculations. One of these approaches is the Importance-Truncated NCSM [4] where the model spaces are extended by using an importance measure evaluated using perturbation theory. Another approach is the Symmetry-Adapted NCSM [5] where the model spaces are truncated by the selected symmetry groups. Similar to these attempts, the no-core Monte Carlo Shell Model (MCSM) [6, 7, 8] is one of the promising candidates to go beyond the Full Configuration Interaction (FCI) method which is a different truncation of the basis states that commonly used in the NCSM.

In these proceedings, we focus on the latest application of the MCSM toward the *ab initio* no-core calculations, which has become viable recently with the aid of major developments in the MCSM algorithm [8, 9, 10] and also a remarkable growth in the computational power of state-of-the-art supercomputers. The overview of the benchmarks in the no-core MCSM is based on the results mostly presented in Refs. [7, 8].

2 MCSM

The MCSM has been developed mainly for conventional shell-model calculations with an assumed inert core [11]. Recently the algorithm and code itself have been heavily revised and rewritten so as to accommodate massively parallel computing environments [8, 9, 10]. In this section, we briefly overview the MCSM and introduce some of recent developments.

2.1 Brief overview

The MCSM approach [11] proceeds through a sequence of diagonalization steps within the Hilbert subspace spanned by the deformed Slater determinants in the HO single-particle basis as the selected importance-truncated bases. A many-body basis state $|\Psi^{J^\pi M}\rangle$ is a linear combination of non-orthogonal angular-momentum (J) and parity (π) projected deformed Slater determinants with good total angular momentum projection (M) as a stochastically selected basis,

$$|\Psi^{J^\pi M}\rangle = \sum_{n=1}^{N_b} f_n \sum_{K=-J}^J g_{nK} P_{MK}^J P^\pi |\phi_n\rangle, \quad (1)$$

where the deformed Slater determinant is $|\phi\rangle = \prod_{i=1}^A a_i^\dagger |-\rangle$ with the vacuum $|-\rangle$ and the creation operator $a_i^\dagger = \sum_{\alpha=1}^{N_{sp}} c_\alpha^\dagger D_{\alpha i}$. N_{sp} is specified by the cutoff of the single particle orbits, N_{shell} . One then stochastically samples the coefficient $D_{\alpha i}$ in all possible many-body basis states around the mean field solutions through the auxiliary fields and diagonalizes the Hamiltonian matrix within the subspace spanned by these bases N_b . Stochastically sampled bases are accepted so as to minimize the energy variationally. Therefore the MCSM can evade the so-called negative sign problem, which is the fundamental issue that cannot be avoided in quantum Monte Carlo methods. With increasing MCSM basis dimension, N_b , the ground state energy of a MCSM calculation converges from above to the exact value. The energy, therefore, always gives the variational upper bound in this framework.

An exploratory no-core MCSM investigation demonstrating a proof-of-the principle has been done for the low-lying states of the Beryllium isotopes by applying the existing MCSM algorithm with a core to a no-core problem [6]. Recent improvements on the MCSM algorithm have enabled significantly larger calculations [8, 9, 10]. We adopt these improvements in the present work [7, 8].

2.2 Recent developments

Among the recently achieved developments of our MCSM algorithm [8, 9, 10], in this subsection, we focus on two improvements: (1) the efficient computation of the two-body matrix elements (TBMEs) for the most time-consuming part in our calculations [8, 9] and (2) the energy-variance extrapolation for our MCSM (approximated) results to the FCI (exact) ones [8, 10]. There are other improvements such as the conjugate gradient method in the process of the basis search and the re-ordering technique in the energy variance extrapolations. Because of space limitations, we refer for the details of these improvements to Refs. [8, 10].

2.2.1 Efficient computation of the TBMEs

One of the main issues in the shell-model calculations is to evaluate TBMEs efficiently. As the matrix for the TBMEs is sparse in general, the indirect-index (list-vector) method is usually adopted in the shell-model calculations by keeping the value of the non-zero matrix elements and their indices. However, it tends to give slow performance due to the irregular memory access patterns.

$$\left(\begin{array}{c} {}^t \tilde{\rho} \end{array} \right) \times \left(\begin{array}{ccccc} & -1 & 0 & +1 & \\ -1 & 0 & \tilde{V} & & \\ 0 & & 0 & & \\ +1 & & & 0 & \end{array} \right) \times \left(\begin{array}{c} \tilde{\rho} \end{array} \right)$$

Figure 1: Schematic illustration of the (vector)^t × (matrix) × (vector) operation.

Alternatively, in our recent MCSM code, we transform the sparse matrix to a block matrix with dense blocks by utilizing the symmetries of the two-body interaction [9]. The one-body density-matrix elements $\rho_{ll'}$ are grouped as $\tilde{\rho}(\Delta m)$ according to $\Delta m \equiv j_z(l') - j_z(l)$ where l and l' are the labels for the state. The TBMEs are also similarly categorized. Then, the two-body part of the Hamiltonian overlap can be expressed as schematically indicated in Fig. 1. Furthermore, most of the computational time is devoted to the (matrix) × (vector) operation. It is usually repeated a number of times for different $\tilde{\rho}$'s. By binding N_{vec} $\tilde{\rho}$ -vectors into a matrix, repeated (matrix) × (vector) operations are replaced by a (matrix) × (matrix) operation at once. As shown in Fig. 2, we can achieve 70–80 % of the peak performance with $N_{\text{vec}} \sim 30–100$ in the test case of the (matrix) × (matrix) operation [9].

2.2.2 Energy-variance extrapolation to the FCI results

With increasing Monte Carlo basis dimension N_b , the MCSM results converge to the FCI results from above. In order to estimate the exact FCI answer, we extrapolate the energy and other observables evaluated by MCSM wave functions using the energy

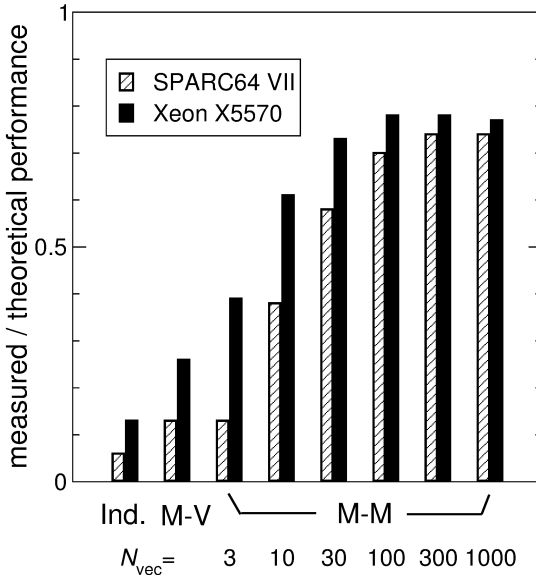


Figure 2: Comparison of the computational performance among the indirect-index method (Ind.), matrix-vector method (M-V) and matrix-matrix method (M-M) with different N_{vec} measured on the SPARC64 VII and Xeon X5570 systems. The values are normalized by their theoretical peak performance. See Ref. [9] for the details.

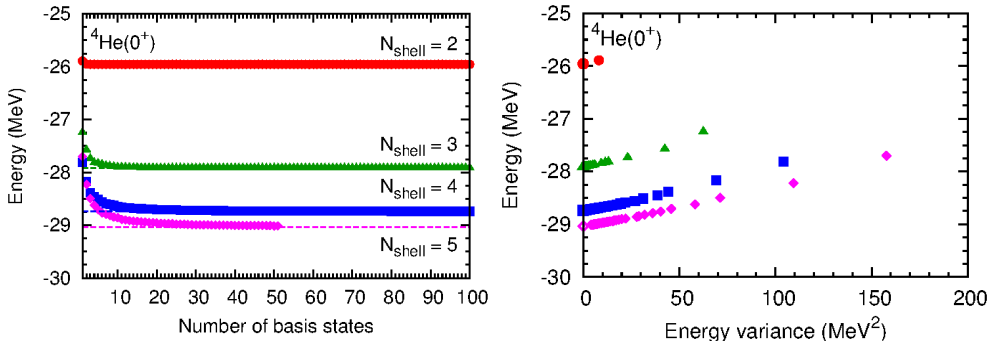


Figure 3: ${}^4\text{He}$ ground-state energies as functions of number of basis states (left) and energy variance (right). From the above to the bottom, the symbols (horizontal dashed lines in the left figure and open symbols at the zero energy variance in the right figure) are the MCSM (FCI) results in $N_{shell} = 2, 3, 4$ and 5 , respectively. See Ref. [7] for the details.

variance [8, 10]. That is, the MCSM results are plotted as a function of the evaluated energy variance, $\Delta E_2 = \langle \Psi | H^2 | \Psi \rangle - (\langle \Psi | H | \Psi \rangle)^2$, and then extrapolated to zero variance.

As a typical example, the behavior of the ground-state energies of ${}^4\text{He}$ (0^+) with respect to the number of basis states and to the energy variance are shown in Fig. 3. From Fig. 3, one can see that the MCSM results can be extrapolated to the FCI ones by using the quadratic fit function of $E(\Delta E_2) = E(\Delta E_2 = 0) + c_1 \Delta E_2 + c_2 (\Delta E_2)^2$ with the fitting parameters $E(\Delta E_2 = 0)$, c_1 , and c_2 .

3 Benchmarks

Augmented by the recent development of the MCSM algorithm [8, 9, 10], we have performed benchmarks of the no-core MCSM calculations [7, 8]. The main outcome of the initial benchmark project is summarized in Table 1. In Table 1, we illustrate the comparisons of the energies for each state and model space between the MCSM and FCI methods. The FCI gives the exact energies in the given model space while the MCSM gives approximate energies. Thus the comparisons between them show how well the MCSM works in no-core calculations. Furthermore, we also put the No-Core Full Configuration (NCFC) [12] results for the states of $4 \leq A \leq 10$ as the fully converged energies in the infinite model space.

For this benchmark comparison, the JISP16 two-nucleon interaction [13] is adopted and the Coulomb force is turned off. Isospin symmetry is assumed. The energies are evaluated for the optimal harmonic oscillator frequencies where the calculated energies are minimized for each state and model space. Here the contributions from the spurious center-of-mass motion are ignored for simplicity.

The comparisons are made for the states; ${}^4\text{He}$ (0^+), ${}^6\text{He}$ (0^+), ${}^6\text{Li}$ (1^+), ${}^7\text{Li}$ ($1/2^-$, $3/2^-$), ${}^8\text{Be}$ (0^+), ${}^{10}\text{B}$ (1^+ , 3^+) and ${}^{12}\text{C}$ (0^+). The model space ranges from $N_{shell} = 2$ to 5 for $A \leq 6$ (4 for $A \geq 7$). Note that the energies of ${}^{10}\text{B}$ (1^+ , 3^+) and ${}^{12}\text{C}$ (0^+) in $N_{shell} = 4$ are available only from the MCSM results. The M -scheme dimensions for these states are already close to or above the current limitation in the FCI approach. The numbers of basis states are taken up to 100 in $N_{shell} = 2-4$ and 50 in $N_{shell} = 5$.

As seen in Table 1, the energies are consistent with each other where the FCI results are available to within ~ 100 keV (~ 500 keV) at most of the MCSM results with(out) the energy-variance extrapolation of the MCSM results. The other

Table 1: Energies in MeV calculated for seven ground states and two excited states within the MCSM and FCI methods using the JISP16 *NN* interaction. The entries of the MCSM indicate the MCSM results before the energy variance extrapolation, while those of the “extrp” line denote the MCSM results after the extrapolations. Uncertainties in extrapolated results are quoted in parenthesis. See Ref. [7] for the details.

Nuclei	Method	<i>E</i> (MeV)				
		<i>N</i> _{shell} = 2	3	4	5	NCFC
⁴ He (0 ⁺)	MCSM	-25.956	-27.914	-28.737	-29.011	-29.164(2)
	extrp			-28.738(1)	-29.037(1)	
	FCI	-25.956	-27.914	-28.738	-29.036	
⁶ He (0 ⁺)	MCSM	-13.343	-19.186	-23.480	-25.080	-29.51(5)
	extrp		-19.196(1)	-23.687(4)	-26.086(76)	
	FCI	-13.343	-19.196	-23.684	-26.079	
⁶ Li (1 ⁺)	MCSM	-14.218	-21.549	-26.757	-28.410	-33.22(4)
	extrp		-21.581(1)	-27.166(16)	-29.873(83)	
	FCI	-14.218	-21.581	-27.168	-29.893	
⁷ Li (1/2 ⁻)	MCSM	-14.459	-24.073	-30.904		-39.8(1)
	extrp		-24.167(2)	-31.780(51)		
	FCI	-14.458	-24.165	-31.748		
⁷ Li (3/2 ⁻)	MCSM	-17.232	-25.978	-32.494		-40.4(1)
	extrp		-26.061(4)	-33.272(89)		
	FCI	-17.232	-26.063	-33.202		
⁸ Be (0 ⁺)	MCSM	-28.435	-41.242	-50.222		-59.1(1)
	extrp		-41.293(1)	-50.753(32)		
	FCI	-28.435	-41.291	-50.756		
¹⁰ B (1 ⁺)	MCSM	-29.755	-41.965	-52.239		-68.5(1.5)
	extrp		-42.357(46)	-54.89(16)		
	FCI	-29.755	-42.338			
¹⁰ B (3 ⁺)	MCSM	-34.221	-46.263	-56.346		-69.8(2)
	extrp		-46.618(22)	-58.41(13)		
	FCI	-34.221	-46.602			
¹² C (0 ⁺)	MCSM	-62.329	-76.413	-90.158		
	extrp		-76.621(4)	-91.957(43)		
	FCI	-62.329	-76.621			

observables besides the energies; the point-particle root-mean-square matter radii and electromagnetic moments also give reasonable agreements between the MCSM and FCI results. The detailed comparisons among the MCSM, FCI, and NCFC methods are discussed in Ref. [7].

4 Summary

By exploiting the recent development in the efficient computation of the Hamiltonian matrix elements between non-orthogonal Slater determinants and the technique of energy-variance extrapolation, the observables give good agreement between the MCSM and FCI results in the *p*-shell nuclei. From the benchmark comparison, the no-core MCSM is now verified in the application to the *ab initio* no-core calculations for light nuclei. The application to heavier nuclei is expected in the near future.

Acknowledgments

This work was supported in part by the SPIRE Field 5 from MEXT, Japan. We also acknowledge Grants-in-Aid for Young Scientists (Nos. 20740127 and 21740204), for Scientific Research (Nos. 20244022 and 23244049), and for Scientific Research on Innovative Areas (No. 20105003) from JSPS, and the CNS-RIKEN joint project for large-scale nuclear structure calculations. This work was also supported in part by the US DOE Grants No. DE-FC02-07ER41457, DE-FC02-09ER41582 (UNEDF SciDAC Collaboration), and DE-FG02-87ER40371, by US NSF grant 0904782, and through JUSTIPEN under grant no. DE-FG02-06ER41407. A part of the MCSM calculations was performed on the T2K Open Supercomputer at the University of Tokyo and University of Tsukuba, and the BX900 Supercomputer at JAEA. Computational resources for the FCI and NCFC calculations were provided by the National Energy Research Supercomputer Center (NERSC), which is supported by the Office of Science of the U.S. Department of Energy under Contract No. DE-AC02-05CH11231, and by the Oak Ridge Leadership Computing Facility at the Oak Ridge National Laboratory, which is supported by the Office of Science of the U.S. Department of Energy under Contract No. DE-AC05-00OR22725.

References

- [1] S. C. Pieper, R. B. Wiringa and J. Carlson, Phys. Rev. C **70**, 054325 (2004); K. M. Nollett, S. C. Pieper, R. B. Wiringa, J. Carlson and G. M. Hale, Phys. Rev. Lett. **99**, 022502 (2007).
- [2] G. Hagen, M. Hjorth-Jensen, G. R. Jansen, R. Machleidt and T. Papenbrock, Phys. Rev. Lett. **108**, 242501 (2012); **109**, 032502 (2012) and references therein.
- [3] P. Navrátil, J. P. Vary and B. R. Barrett, Phys. Rev. Lett. **84**, 5728 (2000); Phys. Rev. C **62**, 054311 (2000); S. Quaglioni and P. Navrátil, Phys. Rev. Lett. **101**, 092501 (2008); Phys. Rev. C **79**, 044606 (2009).
- [4] R. Roth, Phys. Rev. C **79**, 064324 (2009); R. Roth, S. Binder, K. Vobig, A. Calci, J. Langhammer and P. Navrátil, Phys. Rev. Lett. **109**, 052501 (2012).
- [5] T. Dytrych, K. D. Sviratcheva, C. Bahri, J. P. Draayer and J. P. Vary, Phys. Rev. Lett. **98**, 162503 (2007); J. Phys. G. **35**, 095101 (2008); T. Dytrych, K. D. Sviratcheva, J. P. Draayer, C. Bahri and J. P. Vary, *ibid.* **35**, 123101 (2008).
- [6] L. Liu, T. Otsuka, N. Shimizu, Y. Utsuno and R. Roth, Phys. Rev. C **86**, 014304 (2012).
- [7] T. Abe, P. Maris, T. Otsuka, N. Shimizu, Y. Utsuno and J. P. Vary, AIP Conf. Proc. **1355**, 173 (2011); Phys. Rev. C **86**, 054301 (2012).
- [8] N. Shimizu, T. Abe, Y. Tsunoda, Y. Utsuno, T. Yoshida, T. Mizusaki, M. Honma and T. Otsuka, Prog. Theor. Exp. Phys. 01A205 (2012).
- [9] Y. Utsuno, N. Shimizu, T. Otsuka and T. Abe, Comput. Phys. Comm. **184**, 102 (2013).
- [10] N. Shimizu, Y. Utsuno, T. Mizusaki, T. Otsuka, T. Abe and M. Honma, Phys. Rev. C **82**, 061305(R) (2010); N. Shimizu, Y. Utsuno, T. Mizusaki, M. Honma, Y. Tsunoda and T. Otsuka, *ibid.* **85**, 054301 (2012).
- [11] T. Otsuka, M. Honma, T. Mizusaki, N. Shimizu and Y. Utsuno, Prog. Part. Nucl. Phys. **47**, 319 (2001); Y. Utsuno, in *Proc. Int. Workshop*

Nucl. Theor. Supercomputing Era (NTSE-2012), Khabarovsk, Russia, June 18–22, 2012, edited by A. M. Shirokov and A. I. Mazur. Pacific National University, Khabarovsk, 2013 (*see this book*) p. 26.

- [12] P. Maris, J. P. Vary and A. M. Shirokov, Phys. Rev. C **79**, 14308 (2009); P. Maris, A. M. Shirokov and J. P. Vary, *ibid.* **81**, 021301 (2010); C. Cockrell, P. Maris and J. P. Vary, *ibid.* **86**, 034325 (2010).
- [13] A. M. Shirokov, J. P. Vary, A. I. Mazur and T. A. Weber, Phys. Lett. B **644**, 33 (2007); A. M. Shirokov, J. P. Vary, A. I. Mazur, S. A. Zaytsev and T. A. Weber, *ibid.* **621**, 96 (2005).